https://doi.org/10.2352/issn.2169-2629.2021.29.25

Spectral-Reflectance Estimation under Multiple Light Sources

Shoji Tominaga; Norwegian University of Science and Technology, Gjøvik, Norway / Nagano University, Ueda, Japan

Abstract

We describe a comprehensive method for estimating the surface-spectral reflectance from the image data of objects acquired under multiple light sources. This study uses the objects made of an inhomogeneous dielectric material with specular highlights. A spectral camera is used as an imaging system. The overall appearance of objects in a scene results from the chromatic factors such as reflectance and illuminant and the shading terms such as surface geometry and position. We first describe the method of estimating the illuminant spectra of multiple light sources based on detecting highlights appearing on object surfaces. The highlight candidates are detected first, and then some appropriate highlight areas are interactively selected among the candidates. Next, we estimate the spectral reflectance from a wide area selected from an object's surface. The color signals observed from the selected area are described using the estimated illuminant spectra, the surface-spectral reflectance, and the shading terms. This estimation utilizes the fact that the definition domains of reflectance and shading terms are different in each other. We develop an iterative algorithm for estimating the reflectance and the shading terms in two steps repeatedly. Finally, the feasibility of the proposed method is confirmed in an experiment using everyday objects under the illumination environment with multiple light sources.

Introduction

Because the surface-spectral reflectance provides a physical feature inherent to the surface of a target object, knowing the spectral reflectances of objects in a scene is crucial in many aspects such as recognizing and identifying objects, realizing color constancy, and constructing object appearance. The problem of estimating the surface-spectral reflectance from image data has a long history. So far, many methods have been proposed in a variety of fields, including color science, image science and technology, and computer vision (e.g., see [1-5]. When an imaging system observes the reflected light, called color signal [6], from object surfaces illuminated by a light source, the reflectance estimation problem always involves separating illumination and reflectance from the color signal.

In the estimation problem, how to assume the environment illuminating the object surfaces is important. Most methods assumed uniform illumination from a single light source or restricted to a scene in which the illumination across the scene is constant. We note that our illumination environment is not necessarily a single light source nor constant such as daylight or a light bulb. Still, it often consists of multiple light sources from different directions (e.g., see [7-8]).

The present study considers a comprehensive estimation problem that estimates reflectance and illuminant. As a first step towards solving the problem, Tominaga et al.[9] discussed an approach to estimate light sources and their spectral-power distributions from the spectral image data of objects acquired in a complex illumination environment. The target objects were everyday objects, which were usually assumed to be made of an inhomogeneous dielectric material. The illuminant spectra and the corresponding light sources were effectively estimated based on highlight areas on dielectric object surfaces.

We note that multiple light sources generate the illumination field where different locations in a scene possess different spectral-power distributions, which are the mixture of illuminants emitted from the multiple light sources. For instance, we suppose different locations in a room with a ceiling lamp, a table lamp, and daylight through a window.

In addition to the non-uniformity of illuminant spectra, the material making up an object's surface and the object's shape must be taken into consideration when estimating the surface-spectral reflectance. Objects existing in a scene are not necessarily matte and flat objects. In the case of dielectric materials, glosses or specularities may appear on the object surfaces. In curved objects, surface normals may change depending on the location or the surface roughness may differ.

The overall appearance of three-dimensional objects in a scene, results from combining the chromatic factors (such as reflectance and scene illuminant) and the geometric factors (such as surface geometry, roughness, position, and lighting conditions). Although the geometric factors do not have color information, they have shading information, so they may be called shading terms in this paper. They also are sometimes called the geometric factors. In this paper, the color signals observed from an object's surface are modeled using the illuminant spectra, the surface-spectral reflectance, and the shading terms. Since the estimated illuminant spectra are available in the first step, both spectral reflectance and shading terms are the unknowns to be estimated in solving the spectral reflectance estimation problem.

The two unknowns have different domains. That is, spectral reflectance is defined in the wavelength domain, and the shading terms are defined in the spatial coordinate domain. We develop an iterative algorithm that estimates the reflectance and the shading terms in two steps repeatedly, where the output estimates in the first step are used as input in the second step, and the output estimate are then used as input for the other step.

In the following, first, we describe the method of estimating the illuminant spectra based on highlight detection. Next, we consider estimating the spectral reflectance from a wide area selected from an object's surface. The color signals observed from the selected area are described using the estimated illuminant spectra, the surface-spectral reflectance, and the shading terms. We develop an iterative algorithm that estimates the reflectance and the shading terms in two steps repeatedly. Finally, the feasibility of the proposed approach to spectral-reflectance estimation is confirmed in an experiment, where multiple light sources illuminate real dielectric objects.

Illuminant Estimation

A. Highlight detection

Many of the objects we see in our daily lives are plastics, ceramics, natural objects such as fruits, painted metals and wood, and leather products, the surface materials of which are inhomogeneous dielectrics. Light reflection from an inhomogeneous dielectric object consists of specular reflection and diffuse reflection components. The spectral composition of the specular reflection component is the same as that of illumination

light. The specular reflection component often produces gloss and specular highlights. Therefore, if there is gloss or highlight on an object surface, the illumination light source is estimated using it as a clue. In Ref.[9], the illuminant spectra were estimated based on highlight areas appearing on the object surfaces. Highlight areas were detected using a center-surround filter.

Since the present paper purposes to estimate the surface-spectral reflectance of a target object, highlight regions are interactively determined to improve the efficiency of illuminant estimation. In other words, a set of the highlight candidates is detected first. Then some appropriate highlight areas are interactively selected among the set by considering the intensities, locations, and shapes of the highlight candidates. This process is not automated, but needs the manual input.

Let $Y(\mathbf{x},\lambda)$ be the observed color signal (spectral radiance of the reflected light) at pixel location $\mathbf{x}$ = (x, y) from an object surface. The color signals can be recovered from the outputs of a spectral imaging system by knowing the spectral sensitivity functions. We use the luminance value $L(\mathbf{x})$ for highlight detection, which is calculated from the color signal by the CIE luminosity function. A filter creating the center-surround filter is determined by a difference of two Gaussian distributions (DOG) of equal areas. The broader Gaussian is subtracted from the narrower Gaussian. The filter outputs applied to the luminance image $L(\mathbf{x})$ are calculated by a convolution by multiplying pixel values of the luminance image to the matrix over some range.

B. Spectral Estimation

The highlight areas provide an important clue for estimating the light sources. The specular reflection occurs only when the incidence angle of the incoming light is coincident with the viewing angle by a camera. We note that each detected highlight area has the illuminant information of the corresponding only one light source among multiple light sources. The algorithm for estimating illuminant spectra is described. When the object surface consists of an inhomogeneous dielectric material, the color signal is described by the dichromatic reflection model as follows:

$$Y(\mathbf{x},\lambda) = Y_{\mathrm{D}}(\mathbf{x},\lambda) + Y_{\mathrm{S}}(\mathbf{x},\lambda) \tag{1}$$

where the suffix D and S indicate the diffuse reflection component and the specular reflection component, respectively. We suppose L different light sources. Let $S(\lambda)$ be the surface-spectral reflectance of the target object, and let $E(\lambda)$ be the spectral power distribution of the incident light, which is the mixture of different illuminant from L light sources $E(\lambda) = E_1(\lambda) + E_2(\lambda) + \ldots + E_L(\lambda)$. Then the color signal observed at a highlight point $\mathbf{x}_{\mathrm{P}}$ is described as

$$Y(\mathbf{x}_{\mathrm{P}},\lambda) = c_{\mathrm{D}}(\mathbf{x}_{\mathrm{P}})S(\lambda)E(\lambda) + c_{\mathrm{S}}(\mathbf{x}_{\mathrm{P}})E_i(\lambda) \tag{2}$$

where $E_i(\lambda)$ is the illuminant spectrum of a single light source corresponding to the highlight, and $c_{\mathrm{D}}(\mathbf{x}_{\mathrm{P}})$ and $c_{\mathrm{P}}(\mathbf{x}_{\mathrm{P}})$ are the weighting coefficients to the spectral functions, which are constants over the visible wavelength range. We estimate $E_i(\lambda)$ based on the data set of observed spectra $\{Y(\mathbf{x}_{\mathrm{P}},\lambda)\}$ at the highlight area.

The singular-value decomposition (SVD) is applied to the data set at each highlight area [10]. Recently, SVD is often used as a tool for PCA. The SVD provides an orthogonal decomposition of the data matrix of $\{Y(\mathbf{x}_{\mathrm{P}},\lambda)\}$ by using the singular vectors $\mathbf{u}_1, \mathbf{u}_2, \ldots$. The spectral data are then mapped onto a two-dimensional subspace defined by the first two singular vectors $\mathbf{u}_1$ and $\mathbf{u}_2$, due to the characteristic of the dichromatic reflection. Figure 1 shows an example of the pixel distribution, where the coordinates (a_1, a_2) are calculated by the first two singular vectors. Although the pixel distribution appears as a straight line, it consists of two clusters. The pixel distribution on the upper right in the figure mostly belongs to the diffuse cluster, and the remaining linear distribution is the cluster by the specular reflection component. The directional vectors of this linear cluster correspond to the light source color, that is, the illuminant to be estimated. In Figure 1, points A and B are the centroid of the pixel distribution and the farthest pixel point from the centroid A, respectively. The directional vector $\mathrm{A} \rightarrow \mathrm{B}$ of the linear cluster corresponds to the light source color. We note that the linear highlight cluster is much longer than the diffuse cluster. Thus, illuminant estimation is reduced to detecting the direction vector $\mathrm{A} \rightarrow \mathrm{B}$. The spectral curve of the illuminant is estimated from the singular vectors $\mathbf{u}_1$ and $\mathbf{u}_2$, and the directional vector a_2/a_1. We obtain the estimated spectral curve of illuminant at each highlight area.

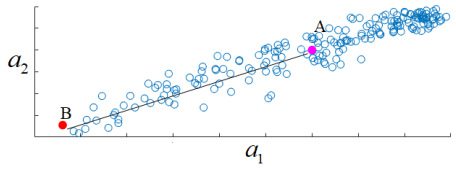

Figure 1 Pixel distribution of the image data in a highlight area projected on the two-dimensional space (a_1, a_2), where the points A and B are the centroid of the pixel distribution and the farthest pixel point from the centroid A, respectively.

Reflectance Estimation

A. Observation model

We consider estimating the spectral reflectance $S(\lambda)$ from a wide area of an object's surface. Figure 2 shows an observation scene by a spectral camera for the reflectance estimation, where an object is illuminated under multiple light sources. A discrete form of the color signal $Y(\lambda,\mathbf{x})$ is often represented as an n-dimensional column vector when the visible range [400-700nm] is sampled at n wavelengths with equal intervals. Typically, in this paper, all spectral functions are sampled in the high dimension of n=61 with 5nm intervals. Let N be the number of pixels in the region of interest. The color signals observed at wavelengths λ_i (i=1, 2, …, n) and pixel points $\mathbf{x}_j$ (j=1, 2, …, N) are described as

$$Y(\lambda_i, \mathbf{x}_j) = c_{S1}(\mathbf{x}_j)E_1(\lambda_i) + c_{S2}(\mathbf{x}_j)E_2(\lambda_i) + \ldots + c_{SN}(\mathbf{x}_j)E_L(\lambda_i) + c_{D1}(\mathbf{x}_j)S(\lambda_i)E_1(\lambda_i) + c_{D2}(\mathbf{x}_j)S(\lambda_i)E_2(\lambda_i) + \ldots + c_{DN}(\mathbf{x}_j)S(\lambda_i)E_L(\lambda_i) \quad (3)$$

We note that the weighting coefficients $c_{Sk}(\mathbf{x}_j)$ and $c_{Dk}(\mathbf{x}_j)$ (k=1, 2, ..., L) are the shading terms, which depend on such geometries as object shape, position, and distance from light and camera. Normally, there are as many shading terms as the two components of specular reflection and diffuse reflection multiplied by the number of light sources

We note that the illuminant spectral $E_k(\lambda)$ (k=1, 2, ..., L) of L light sources are already estimated in the previous section. The spectral reflectance $S(\lambda)$ and the shading terms $c_{Sk}(\mathbf{x}_j)$ and $c_{Dk}(\mathbf{x}_j)$ (k=1, 2, ..., L) are unknown to be estimated. We define several vectors for discrete representation of the model as follows:

$$\mathbf{s} = \begin{bmatrix} S(\lambda_1) \\ S(\lambda_2) \\ \vdots \\ S(\lambda_n) \end{bmatrix}, \quad \mathbf{y}_j = \begin{bmatrix} y(\lambda_1, \mathbf{x}_j) \\ y(\lambda_2, \mathbf{x}_j) \\ \vdots \\ y(\lambda_n, \mathbf{x}_j) \end{bmatrix}, \quad \mathbf{c}_j = \begin{bmatrix} c_{S1}(\mathbf{x}_j) \\ \vdots \\ c_{SL}(\mathbf{x}_j) \\ c_{D1}(\mathbf{x}_j) \\ \vdots \\ c_{DL}(\mathbf{x}_j) \end{bmatrix},$$

$$\mathbf{z}_i = \begin{bmatrix} y(\lambda_i, \mathbf{x}_1) - c_{S1}(\mathbf{x}_1)E_1(\lambda_i) - \ldots - c_{SL}(\mathbf{x}_1)E_L(\lambda_i) \\ y(\lambda_i, \mathbf{x}_2) - c_{S1}(\mathbf{x}_2)E_1(\lambda_i) - \ldots - c_{SL}(\mathbf{x}_2)E_L(\lambda_i) \\ \vdots \\ y(\lambda_i, \mathbf{x}_N) - c_{S1}(\mathbf{x}_N)E_1(\lambda_i) - \ldots - c_{SL}(\mathbf{x}_N)E_L(\lambda_i) \end{bmatrix},$$

$$(i = 1, 2, \ldots, n, \quad j = 1, 2, \ldots, N) \quad (4)$$

where $\mathbf{s}$ is an n-dimensional column vector of the spectral reflectance, $\mathbf{y}_j$ is an n-dimensional column vector of the imaging system outputs at location $\mathbf{x}_j$, $\mathbf{c}_j$ is a 2L-dimensional column vector of the shading terms at location $\mathbf{x}_j$, and $\mathbf{z}_i$ is an N-dimensional observation vector for diffuse reflection component at wavelength λ_i, which is obtained by subtracting the specular reflection component from the observation.

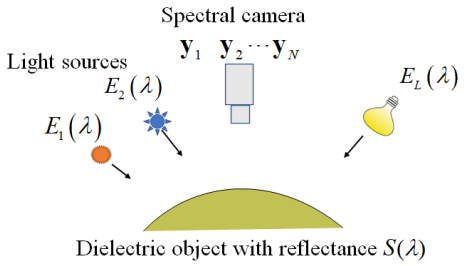

Figure 2 Observation scene by a spectral camera for the reflectance estimation.

B. Estimation algorithm

Because there are two types of unknown variables s and $\mathbf{c}_j$, in this paper, we propose an iterative solution method to obtain the optimal estimates of the surface-spectral reflectance function and all weighting coefficients of the shading terms. The iterative process is decomposed into two steps of (1) the estimates of the shading terms are updated under the estimated reflectance fixed and (2) the estimate of the reflectance is updated under the estimated shading terms fixed.

(1) Shading term estimation

The relationship between the shading terms and all observations is described as

$$\begin{bmatrix} \mathbf{y}_1 \\ \mathbf{y}_2 \\ \vdots \\ \mathbf{y}_N \end{bmatrix} = \begin{bmatrix} \mathbf{B} & \mathbf{0} & \cdots & \mathbf{0} \\ \mathbf{0} & \mathbf{B} & \ddots & \vdots \\ \vdots & \ddots & \ddots & \mathbf{0} \\ \mathbf{0} & \cdots & \mathbf{0} & \mathbf{B} \end{bmatrix} \begin{bmatrix} \mathbf{c}_1 \\ \mathbf{c}_2 \\ \vdots \\ \mathbf{c}_N \end{bmatrix}, \quad (5)$$

where the observation vector in the left side is an nN-dimensional vector, an $n \times 2L$ matrix $\mathbf{B}$ in the right side is defined as

$$\mathbf{B} = \begin{bmatrix} E_1(\lambda_1) & \cdots & E_L(\lambda_1) & S(\lambda_1)E_1(\lambda_1) & \cdots & S(\lambda_1)E_L(\lambda_1) \\ E_1(\lambda_2) & \cdots & E_L(\lambda_2) & S(\lambda_2)E_1(\lambda_2) & \cdots & S(\lambda_2)E_L(\lambda_2) \\ \vdots & & \vdots & \vdots & & \vdots \\ E_1(\lambda_n) & \cdots & E_L(\lambda_n) & S(\lambda_n)E_1(\lambda_n) & \cdots & S(\lambda_n)E_L(\lambda_n) \end{bmatrix} \quad (6)$$

The observation at each pixel point is rewritten as

$$\mathbf{y}_j = \mathbf{B}\mathbf{c}_j. \quad (j=1, 2, \ldots, N) \quad (7)$$

Therefore, the standard least square estimate for $\mathbf{c}_j$ is given in a form

$$\hat{\mathbf{c}}_j = \left(\mathbf{B}^t\mathbf{B}\right)^{-1}\mathbf{B}^t\mathbf{y}_j, \quad (j=1, 2, \ldots, N) \quad (8)$$

where symbol *t* represents matrix transposition.

(2) Spectral reflectance estimation

The relationship between the spectral reflectance and all observations is described as

$$\begin{bmatrix} \mathbf{z}_1 \\ \mathbf{z}_2 \\ \vdots \\ \mathbf{z}_n \end{bmatrix} = \begin{bmatrix} \mathbf{b}_1 & \mathbf{0} & \cdots & \mathbf{0} \\ \mathbf{0} & \mathbf{b}_2 & \ddots & \vdots \\ \vdots & \ddots & \ddots & \mathbf{0} \\ \mathbf{0} & \cdots & \mathbf{0} & \mathbf{b}_n \end{bmatrix} \begin{bmatrix} S(\lambda_1) \\ S(\lambda_2) \\ \vdots \\ S(\lambda_n) \end{bmatrix} \tag{9}$$

where the observation vector in the left side is an nN-dimensional vector, an $n \times 1$ matrix $\mathbf{b}_i$ in the right side is defined as

$$\mathbf{b}_i = \begin{bmatrix} c_{D1}(\mathbf{x}_1)E_1(\lambda_i) + c_{D2}(\mathbf{x}_1)E_2(\lambda_i) + \cdots + c_{DL}(\mathbf{x}_1)E_L(\lambda_i) \\ c_{D1}(\mathbf{x}_2)E_1(\lambda_i) + c_{D2}(\mathbf{x}_2)E_2(\lambda_i) + \cdots + c_{DL}(\mathbf{x}_2)E_L(\lambda_i) \\ \vdots \\ c_{D1}(\mathbf{x}_N)E_1(\lambda_i) + c_{D2}(\mathbf{x}_N)E_2(\lambda_i) + \cdots + c_{DL}(\mathbf{x}_N)E_L(\lambda_i) \end{bmatrix}. \tag{10}$$

The observation at each wavelength is rewritten as

$$\mathbf{z}_i = \mathbf{b}_i S(\lambda_i). \qquad (i=1, 2, \ldots, n) \tag{11}$$

Therefore, the standard least square estimate for $\mathbf{s}$ is given in a form

$$\hat{S}(\lambda_i) = \mathbf{b}_i^t \mathbf{z}_i \Big/ \left(\mathbf{b}_i^t \mathbf{b}_i \right). \qquad (i=1, 2, \ldots, n) \tag{12}$$

where we note the estimate is a scalar.

(3) Iterative estimation process

We repeat the iterative estimation calculations of the above two steps (1) and (2), starting from an appropriate initial estimate of spectral reflectance. Figure 3 shows a visual diagram of the iterative estimation process. The initial value of $\hat{S}(\lambda_i)$ is constant in the range $400 \le \lambda \le 700$ (say, $\hat{S}(\lambda_i)$ =0.5). In the observation model Eq.(3), the shading term $c_{Dk}(\mathbf{x})$ (k=1, 2,…, L) and the spectral reflectance $S(\lambda)$ are in a multiplying relationship $c_{Dk}(\mathbf{x})S(\lambda)$. We cannot determine the absolute value of each estimate. Therefore, we assume in this paper that the spectral reflectance is normalized as $\sum_{i=1}^{n} S(\lambda_i)^2 = 1$ ($\|\mathbf{s}\| = 1$).

The area selected for reflectance estimation may affect the performance. Because we aim to estimate the spectral reflectance for the diffuse reflection component, only matte areas containing neither gloss nor specularity can be extracted and used for the estimation. In this case, the specular shading terms $c_{Sk}(\mathbf{x})E_k(\lambda)$ (k=1, 2, ..., L) in the above algorithm are neglected as $c_{Sk}(\mathbf{x}) = 0$. Nevertheless, the rest of the paper describes the general situation where region of interest has both diffuse and specular reflection.

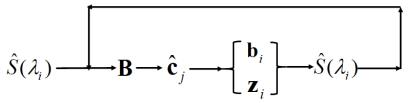

i=1, 2, .., n. j=1, 2, …, N

Figure 3 Visual diagram of the iterative estimation process.

Experimental Results

A. Experimental setup

Figure 4 shows a scene comprising of three objects, where the left object is a blue cylinder made of painted metal, the center object is red paprika of natural product, and the right object is a yellow soy sauce container made of ceramic. These objects were placed on a black felt cloth and illuminated using three different light sources: incandescent light source from a light bulb from the left direction, fluorescent light source from a table lamp from the right direction, and LED light source from a ceiling lamp from the upper direction. The distances between the light sources and the target objects were 1-3 m. Gloss and specular reflection can be seen on the surface of each object. A spectral imaging system was used in experiments, which consisted of a monochrome CCD camera with 12-bit dynamic range and Peltier cooling (QImaging, Retiga 1300), a VariSpec liquid crystal tunable filter, an IR-cut filter, and a personal computer. The imaging system was placed at the same height as the objects and bout 3 m away.

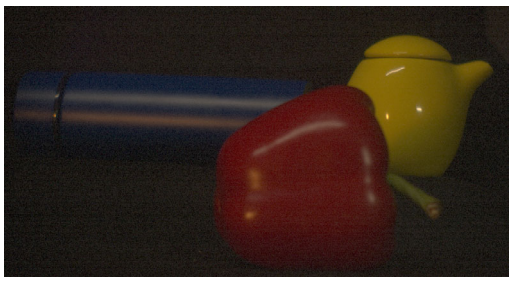

Figure 4 Scene comprising three objects, where the left object is a blue cylinder made of painted metal, the center object is red paprika of natural product, and the right object is a yellow soy sauce container made of ceramic.

B. Illuminant estimation

The spectral image captured from the scene was converted into the luminance image, to which the center-surround filter was applied. Figure 5 (a) shows the filtration outputs by the center-surround filter with $\sigma_1 = 3$ and $\sigma_2 = 7$, and the candidate highlight areas extracted by thresholding. The extracted blue areas in Figure 5 (a) include the boundary area. We then selected specular highlight areas with strong intensity except for the boundary regions. Figure 5 (b) depicts the whole set of eight highlight areas extracted from three object surfaces.

The spectral power distribution was estimated for each of the detected highlight areas. The SVD was applied to the data set of the

observed spectra at each highlight area. The spectral data are then mapped onto a plane defined by the two singular vectors. Eight illuminant spectral curves were estimated at the eight highlight areas along with algorithm in Section **2.2**. Finally, the light source for each highlight and the corresponding spectral power distribution were determined from the clustering algorithm and the iterative labeling process. Figure 6 draws the spectral curves estimated for three light sources, where three bold curves correspond to the estimated illuminant spectra of incandescent, fluorescent, and LED light sources. The method of probabilistic relaxation labeling was applied to identify the three light sources [9]. The broken curves represent the directly measured illuminant spectral power distributions.

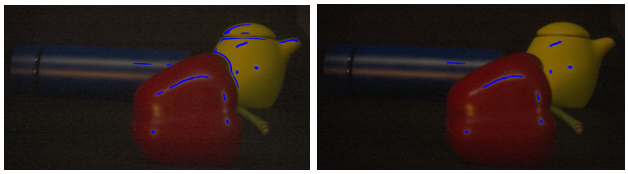

(a) (b)

Figure 5 Highlight detection, where (a) filtration outputs by the center-surround filter, and (b) selected highlight areas with strong intensity except for the boundary regions.

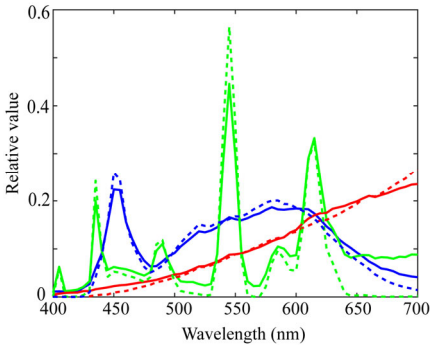

Figure 6 Spectral curves estimated for three light sources, where three bold curves correspond to the estimated illuminant spectra of incandescent, fluorescent, and LED light sources. The broken curves represent the directly measured illuminant spectral power distributions.

C. Reflectance estimation

The red paprika was selected as a target object to examine the performance of spectral reflectance estimation. All spectral functions, including spectral reflectance, illuminant spectra, and output color signals were represented in 61-dimensional column vectors. The number of light sources was L=3, and the estimated spectral curves in Figure 6 were used for the reflectance estimation.

First, the image region used for estimating the spectral reflectance was determined. Region A surrounded by the dashed square in Figure 7, contains many highlights on the red paprika. The region size was about 250x350 pixels, and so the number of pixels N used for reflectance estimation was about 75000 (=250x350). The spectral reflectance and the shading terms were estimated using the proposed algorithm in the previous section. Figures 8 and 9 show the results of 100 iterative calculations. The estimated shading terms for the specular reflection component and the estimated shading terms for the diffuse reflection component are presented in Figure 8, where ($c_{S1}(\mathbf{x})$, $c_{D1}(\mathbf{x})$) , ($c_{S2}(\mathbf{x})$, $c_{D2}(\mathbf{x})$) , and ($c_{S3}(\mathbf{x})$, $c_{D3}(\mathbf{x})$) represent, respectively, the shading terms for (1) the ceiling lamp from the upper direction, (2) the table lamp from the right direction, and (3) the incandescent lamp from the left direction. The gamma correction was applied to the shading images for the specular component to improve the visibility. The mapping between the shading terms and the light sources was done manually here, but the automated mapping is possible because the directions of the light sources can be predicted. We note that the shading images of $c_{S1}(\mathbf{x})$, $c_{S2}(\mathbf{x})$, and $c_{S3}(\mathbf{x})$ contain highlights by the corresponding light sources. Also, note that the shading image of $c_{D3}(\mathbf{x})$ looks brighter than the others. This means that the illumination from the left is stronger compared with the other light sources.

The estimated spectral reflectance of the red paprika is presented by the bold curve (A) in Figure 9. The CIE-LAB color coordinates under white illuminant E with equal energy were L*=21.2, a*=46.7, and b*=-1.8. The dashed curve in Figure 9 represents the directly measured spectral reflectance by a spectrometer, which was used as the ground truth. The root-mean-square error to the ground truth was *rmse*=0.030, and the CIE-LAB color differences were DE76=8.12 and DE00=5.24.

Next, the spectral reflectance was estimated using the image region B without highlights on the red paprika. Region B surrounded by the bold square in Figure 8, contains no highlight at all. This region looks like a uniform color region without gradation of shading and color. However, although the region is not large, it is influenced by the locally non-uniform spatial distributions of the three illuminations. The region size of B was about 120x170 pixels, so that N was about 20400 (=120x170). The estimated spectral reflectance is shown by the broken curve (B) in Figure 10. The root-mean-square error to the ground truth was rmse=0.038, and the CIE-LAB color differences were DE76=2.39 and DE00=1.76.

The same experiment on reflectance estimation was performed for the blue metal cylinder and the yellow ceramic container. We found that the matte regions without specularity are more stable for reflectance estimation than the regions including specularity.

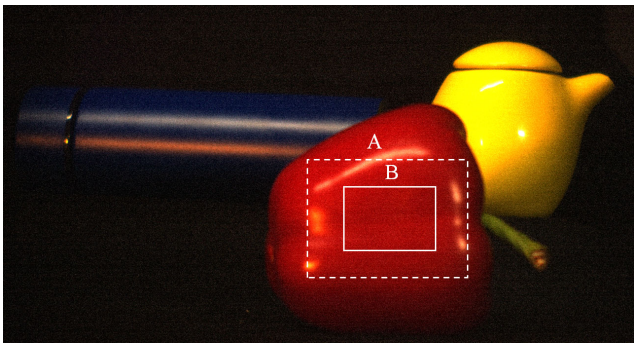

Figure 7 Image regions used for estimating the spectral reflectance of the red paprika, where region A surrounded by the dashed square contains many highlights, and region B surrounded by the bold square contains no highlight at all.

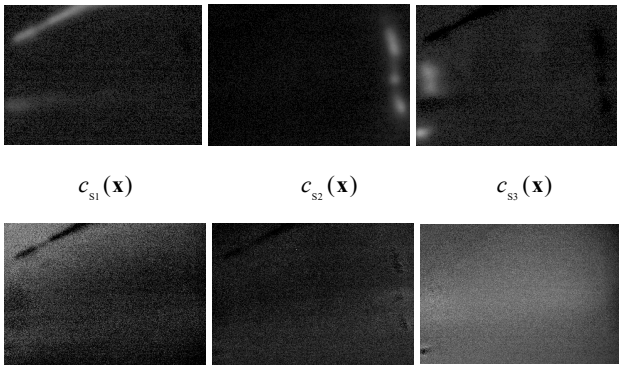

Figure 8 Estimated shading terms $c_{S1}(\mathbf{x})$, $c_{S2}(\mathbf{x})$, and $c_{S3}(\mathbf{x})$ for the specular reflection component and $c_{D1}(\mathbf{x})$, $c_{D2}(\mathbf{x})$, and $c_{D3}(\mathbf{x})$ for the diffuse reflection component for region A. The gamma correction (γ=2.3) was applied to the shading images for the specular component to improve the visibility.

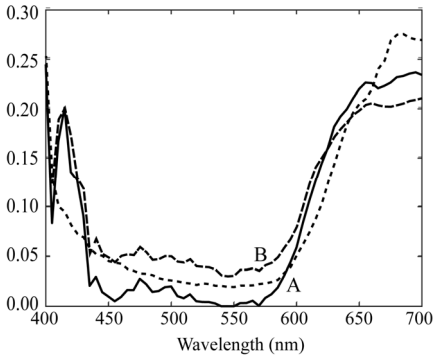

Figure 9 Estimated spectral reflectances of the red paprika, where the bold curve (A) and the broken curve (B) were results from region A and region B in Figure 7, respectively. The dashed curve represents the directly measured spectral reflectance used as the ground truth.

Conclusions

This paper discussed a comprehensive method for estimating the surface-spectral reflectance from the image data of objects acquired under multiple light sources. The target objects were everyday objects, which were usually assumed to be made of an inhomogeneous dielectric material. We supposed the use of a spectral camera as an imaging system. It was noted that the overall appearance of objects in a scene depended on the combination of the chromatic factors such as reflectance and illuminant and the shading terms such as surface geometry and position. The chromatic factors were then represented as spectral functions in the visible range. The shading terms were then represented as position functions in the spatial location range.

We first described the method of estimating the illuminant spectra of multiple light sources based on detecting highlights appearing on object surfaces in a scene. A set of the highlight candidates was detected first, and then some appropriate highlight areas were interactively selected among the set by considering the intensities, locations, and shapes. Next, we considered estimating the spectral reflectance from a wide area selected from an object's surface. The color signals observed from the selected area were described using the estimated illuminant spectra, the surface-spectral reflectance, and the shading terms. The estimation was based on using the fact that the definition domains of reflectance and shading terms were differed. We developed an iterative algorithm for estimating the reflectance and the shading terms in two steps repeatedly. The algorithm could be simplified if the selected area belonged to a matte surface with only a diffuse reflection component without gloss nor highlight.

We experimented to confirm the feasibility of the proposed method using three dielectric objects of painted metal, a natural plant, and ceramic, and an actual illumination environment with multiple light sources of LED, fluorescence, and incandescent. We showed the effectiveness of the proposed estimation algorithm and the accuracy of the estimated illuminant spectra and spectral reflectance compared with the ground truths of the direct measurements.

Acknowledgments

The author would like to Prof. Emeritus Hideaki Sakai at Kyoto University for the useful discussions. This work was supported by JSPS KAKENHI Grant Number JP20K11893.

References

[1] L. Maloney and B. Wandell, “Color constancy: a method for recovering surface spectral reflectance,” J. Optical Society of America A, Vol. 3, No. 1, pp. 29–33 (1986).

[2] S. Tominaga, “Multichannel vision system for estimating surface and illuminant functions,” J. Optical Society of America A, Vol.13, No.11, pp. 2163-2173 (1996).

[3] V. Heikkinen, R. Lenz, T. Jetsu, J. Parkkinen, M. Hauta-Kasari, and T. Jääskeläinen, “Evaluation and unification of some methods for estimating reflectance spectra from RGB images,” J. Optical Society of America A, Vol.25, No.10, pp.2444-2458 (2008)

[4] H. Blasinski, J. Farrell, and B.Wandell, “Simultaneous surface reflectance and fluorescence spectra estimation,” IEEE Trans. Image Process. Vo.29, pp.8791–8804 (2020).

[5] L. Wang, X. Wan, G. Xiao, and J. Liang, “Sequential adaptive estimation for spectral reflectance based on camera responses”, Optics Express, Vol. 28, No. 18, pp.25830-25842 (2020).

[6] B. A. Wandell, Foundation of Vision, Sinauer Associates, Sunderland, MA, 1995), p. 281.

[7] K. Hara, K. Nishino, and K. Ikeuchi, ``Multiple light sources and reflectance property estimation based on a mixture of spherical distributions," Proc. ICCV (IEEE, Piscataway, NJ, 2005), Vol. II, pp. 1627_1634.

[8] A. Gijsenij, R. Lu, and T. Gevers, ``Color constancy for multiple light sources," IEEE Trans. IP, Vol.21, pp. 697_707 (2012).

[9] S. Tominaga, K. Hirai, and T. Horiuchi, “Spectral estimation of multiple light sources based on highlight detection,” J. Imaging Science and Technology, Vol.64, No.5, pp.050408-1_050408-9 (2020).

[10] G. H. Golub and C. F. Van Loan, Matrix Computations (Fourth ed.), Johns Hopkins University (2013).

Author’s Biography

Shoji Tominaga received the B.E., M.S., and Ph.D. degrees in electrical engineering from Osaka University, Japan. He was a Professor (2006-2013) and Dean (2011-2013) at Graduate School in Chiba University. He is now an Adjunct Professor, Norwegian University of Science and Technology and also a Visiting Researcher, Nagano University. His research interests include multispectral imaging, and material appearance. He is a Fellow of IEEE, IS&T, SPIE, and OSA.